Національна академія наук України

ІНСТИТУТ ФІЗИКИ КОНДЕНСОВАНИХ СИСТЕМ ім. І.Р. ЮХНОВСЬКОГО

ICMP–25–02E

O. Baran, T. Verkholyak, T. Krokhmalskii, D. Yaremchuk,
T. Hutak, O. Derzhko

ELECTROMAGNETIC WAVE PROPAGATION
IN ONE-DIMENSIONAL MAGNETOELECTRIC CRYSTAL.
PRELIMINARY NOTES

ЛЬВІВ

УДК: 537.9; 537.622

PACS: 75.10.-b

Поширення електромагнітної хвилі в одновимірному магнетоелектричному кристалі. Попередні нотатки

О. Баран, Т. Верхоляк, Т. Крохмальський, Д. Яремчук, Т. Гутак, О. Держко

Анотація. Ми розглядаємо просту модель одновимірного магнетоелектричного кристала і досліджуємо поширення електромагнітної хвилі через таке середовище. Обчислення дисперсійного співвідношення $\boldsymbol{k}(\omega)$ дозволяє нам проілюструвати, як можна контролювати поширення електромагнітної хвилі магнітним чи електричним полем. Ми демонструємо явно напрямову необоротність, тобто, різницю у поширенні електромагнітної хвилі у протилежних напрямках. Наші строгі обчислення повинні бути корисними для більш реалістичних (але менш математично податливих) моделей магнетоелектричних середовищ.

Electromagnetic wave propagation in one-dimensional magnetoelectric crystal. Preliminary notes

O. Baran, T. Verkholyak, T. Krokhmalskii, D. Yaremchuk, T. Hutak, O. Derzhko

Abstract. We consider a simple model of one-dimensional magnetoelectric crystal and examine the propagation of an electromagnetic wave through such a medium. Calculating the dispersion relation $\boldsymbol{k}(\omega)$ allows us to illustrate how the spread of the electromagnetic wave can be controlled by a magnetic/electric field. We demonstrate explicitly the directional nonreciprocity, i.e., the difference in the electromagnetic wave propagation between opposite directions. Our rigorous calculations should be useful for more realistic (and less tractable mathematically) models of magnetoelectric media.

Препринти Інституту фізики конденсованих систем імені І.Р. Юхновського НАН України доступні на WWW-сервері інституту за адресою https://icmp.lviv.ua/

The preprints of the Yukhnovskii Institute for Condensed Matter Physics of the National Academy of Sciences of Ukraine are available from Institute's WWW server (https://icmp.lviv.ua/en)

Остап Романович Баран
Тарас Михайлович Верхоляк
Тарас Євстахійович Крохмальський
Дмитро Любомирович Яремчук
Тарас Ігорович Гутак
Олег Володимирович Держко

Поширення електромагнітної хвилі в одновимірному магнетоелектричному кристалі. Попередні нотатки

Роботу отримано 29 грудня 2025 р.

Затверджено до друку Вченою радою ІФКС ім. І.Р. Юхновського НАН України

Рекомендовано до друку відділом квантової статистики

Виготовлено при ІФКС ім. І.Р. Юхновського НАН України

We dedicate this work to the memory of Johannes Richter.

1. Introduction

Magnetoelectrics attract much attention nowadays because of possibility to control magnetization/polarization by electric/magnetic field. Several microscopic mechanisms that provide insights into magnetoelectric effect are known nowadays. Among them is the so-called Katsura-Nagaosa-Balatsky (KNB) mechanism, which explains magnetoelectric coupling in Mott insulators.

It might be useful to recall here the main arguments of Katsura, Nagaosa, and Balatsky [1]. They considered a typical electronic model concentrating on the electron levels of a $3d$-transition metal in the octahedral ligand field and in the presence of the on-site spin-orbit interaction. The emerged here two-fold degenerate states further undergo the on-site Hubbard repulsion (treated at a mean-field level) and, as a result, split into two bases states representing the transition metal ion. Next, the authors considered a bond between two transition metal ions through the oxygen connecting them, introduced the Hamiltonian for the electron hopping as a perturbation, and obtained the lowest lying states. Finally, they calculated the expected value of the electric polarization of the metal-metal exchange bond in two cases: The double-exchange interaction and the super-exchange interaction [2]. In both cases, the expected value of the polarization $\boldsymbol{p}_{12}$ is nonzero and is given by

$$\boldsymbol{p}_{12} \propto [\boldsymbol{e}_{12} \times [\boldsymbol{s}_1 \times \boldsymbol{s}_2]] \tag{1}$$

where $\boldsymbol{e}_{12}$ is the unit vector connecting two transition metal ions and $\boldsymbol{s}_1$ and $\boldsymbol{s}_2$ are the electronic spin operators at sites 1 and 2. In both cases, the spin current $\boldsymbol{j}_{12} \propto [\boldsymbol{s}_1 \times \boldsymbol{s}_2]$, therefore one arrives at the conclusion that the spin current $\boldsymbol{j}_{mn}$ flowing between the magnetic sites with spins $\boldsymbol{s}_m$ and $\boldsymbol{s}_n$, $\boldsymbol{j}_{mn} \propto [\boldsymbol{s}_m \times \boldsymbol{s}_n]$, leads to the electric polarization

$$\boldsymbol{p}_{mn} \propto [\boldsymbol{e}_{mn} \times \boldsymbol{j}_{mn}], \tag{2}$$

where $\boldsymbol{e}_{mn}$ is the unit vector pointing from mth site to nth site. A rough estimate on the order of magnitude for $\boldsymbol{p}$ involves the lattice constant, the hopping integral, as well as the energies of oxygen and transition metal orbitals, but after all it may be comparable to experimental data. In the presence of an external electric field $\boldsymbol{E}$, each bond contributes to Hamiltonian the term $-(\boldsymbol{p}_{mn} \cdot \boldsymbol{E})$ and a possibility of the electric (magnetic)

control of magnetic (electric) properties emerges. Many more papers have appeared until now in this field [3–8].

Consider, as an example of magnetoelectric crystal, the Heisenberg chain with the Hamiltonian $H_{XXX} = J\sum_n \boldsymbol{s}_n\cdot\boldsymbol{s}_{n+1}$ and $\boldsymbol{e}_{n,n+1} = (1,0,0)$. Then, according to Eq. (1),

$$\begin{aligned} p^x_{n,n+1} &= 0,\\ p^y_{n,n+1} &\propto -\left(s^x_n s^y_{n+1} - s^y_n s^x_{n+1}\right),\\ p^z_{n,n+1} &\propto -\left(s^x_n s^z_{n+1} - s^z_n s^x_{n+1}\right). \end{aligned} \tag{3}$$

On the other hand, according to Eq. (2), $\boldsymbol{p}_{n,n+1} \propto (0, -j^z_{n,n+1}, j^y_{n,n+1})$ and after calculation the spin-current operator from the continuity equation $\mathrm{d}s^\alpha_n/\mathrm{d}t = -\mathrm{i}[s^\alpha_n, H_{XXX}] = -\mathrm{div} j^\alpha_n = -(j^\alpha_{n,n+1} - j^\alpha_{n-1,n})$, one finds

$$\begin{aligned} p^x_{n,n+1} &= 0,\\ p^y_{n,n+1} &\propto -J\left(s^x_n s^y_{n+1} - s^y_n s^x_{n+1}\right),\\ p^z_{n,n+1} &\propto J\left(s^z_n s^x_{n+1} - s^x_n s^z_{n+1}\right), \end{aligned} \tag{4}$$

see Ref. [9, 10]. Furthermore, the polarization (dipole moment) of the bond $\boldsymbol{p}_{n,n+1}$ couples to an external electric field $\boldsymbol{E}$ with nonzero components in the plane orthogonal to the chain and thus electric control of magnetic properties as well as the magnetic control of electric properties is possible.

The KNB scenario for emerging of magnetoelectricity has been incorporated into some exactly solvable quantum chain models [9–15]. For instance, consider a spin-1/2 XY chain [16] and assume that this model arises from a more fundamental electronic model for which the KNB scenario holds. This means that the electric polarization of the bond between the neighboring sites $\boldsymbol{p}_{n,n+1}$ is determined by Eq. (1) or by the spin current $\boldsymbol{j}_{n,n+1}$ according to Eq. (2). As above, it is convenient to assume that the chain runs along the x-direction in the real space, i.e., $\boldsymbol{e}_{n,n+1} = (1,0,0)$, and that the x-, y-, and z-axis in the real space and in the spin space coincide. Then the bond polarization has zero x-component. Moreover, after calculating the spin-current operator $\boldsymbol{j}_{n,n+1}$ from the lattice version of the continuity equation one concludes that the model remains a free-fermion one if an external uniform electric field is aligned along y-axis. More discussion about such exactly solvable KNB models of magnetoelectrics (including a free-fermion model with three-spin interactions, which may show a nontrivial magnetoelectric effect, i.e., magnetization (polarization) can be induced and governed solely by electric (magnetic) field [11]) can be found in Refs. [9–13, 15]. The main

worth of these models is their exact solvability: All relevant quantities can be calculated rigorously and examined in great detail so that such calculations may serve as a benchmark for more realistic and complicated cases which are not amenable to rigorous solutions.

In the present paper we consider a quantum spin-1/2 chain with the KNB mechanism for magnetoelectricity. Our goal is to illustrate *a magnetoelectric response of the model to oscillating electric and magnetic fields*. To this end, we study electromagnetic wave propagation in the considered magnetoelectric crystal.

It is worthwhile to discuss already at the beginning the scales relevant for this problem. The energy scale is dictated by the exchange coupling, which may vary, say, between $J/k_\mathrm{B} = 10$ K and $J/k_\mathrm{B} = 100$ K (here k_B is the Boltzmann constant). Equating J to $h\nu$ (here h is the Planck constant) we get $\nu \approx 0.208 - 2.084$ terahertz that according to the relation $\lambda = c/\nu$ corresponds to the wavelength $\lambda \approx 1.44 - 0.14$ mm. Furthermore, since the interatomic distance is about a nanometer, i.e., it is several orders smaller than λ, the spin-lattice model weakly couples, as a matter of fact, to spatially uniform electric and magnetic fields of the electromagnetic wave. In other words, only the $\kappa \to 0$ Fourier mode of the spin-lattice system is relevant for the electromagnetic wave propagation under investigation. In our theoretical calculations below we often set $\hbar = h/(2\pi) = 1$ and $k_\mathrm{B} = 1$ for brevity.

The paper is organized as follows. In Sections 2 and 3, we briefly introduce the model and recall the standard treatment of electromagnetic wave propagation through a medium. Section 4 concerns dynamic susceptibilities which enter the formulas for dispersion relation and determine the electromagnetic wave propagation. We discuss and summarize our findings in Section 5. Some side material are delegated to appendices.

2. Simple model of magnetoelectrics

In what follows we consider an N-site spin-1/2 chain augmented by the KNB mechanism with the following Hamiltonian:

$$\begin{aligned} H = &\sum_n J\left(s^x_n s^x_{n+1} + s^y_n s^y_{n+1} + \Delta s^z_n s^z_{n+1}\right)\\ &-\mathcal{E}\sum_n p^y_{n,n+1} - \mathcal{B}\sum_n m^z_n,\\ p^y_{n,n+1} = p_0\left(s^x_n s^y_{n+1} - s^y_n s^x_{n+1}\right),&\quad m^z_n = m_0 s^z_n. \end{aligned} \tag{5}$$

Here, J is the nearest-neighbor interaction (below, we often set $J = 1$ to fix the units), $\Delta = 0$ corresponds to the isotropic XY interaction,

whereas $\Delta = 1$ corresponds to the (isotropic) Heisenberg interaction. Furthermore, the electric field is $\boldsymbol{E} = (0, \mathcal{E}, 0)$, $\mathcal{E} \geq 0$ and the magnetic field is $\boldsymbol{B} = (0, 0, \mathcal{B})$, $\mathcal{B} \geq 0$. Besides, p_0 stands for the electric dipole moment and m_0 (usually, $m_0{=}g\mu_{\rm B}s$, $s{=}1/2$, g is about 2) stands for the magnetic dipole moment; both are inherent in the problem. Sometimes the electric and magnetic fields incorporate p_0 and m_0, respectively, but introducing them explicitly might be helpful in what follows.

To describe a nontrivial magnetoelectric effect, we may add to the Hamiltonian in Eq. (5), e.g., the three-spin $XZY{-}YZX$ interaction, $H \to H + J' \sum_n (s_n^x s_{n+1}^z s_{n+2}^y - s_n^y s_{n+1}^z s_{n+2}^x)$, where J' stands for the three-spin $XZY{-}YZX$ interaction constant [11], see also Appendix A. However, such extra terms are not in the focus of present study.

Various properties of the introduced model with $\Delta = 0$ can be examined rigorously, without making any approximation, by using the standard Jordan-Wigner fermionization method [16]; the interested reader should consult Ref. [11] to gain all details. In brief, after applying the Jordan-Wigner transformation, $c_n = (-2s_1^z)\dots(-2s_{n-1}^z)s_n^-$, and the Fourier transformation, $c_\kappa = \sum_n e^{{\rm i}\kappa n} c_n/\sqrt{N}$, Eq. (4) can be cast into the Hamiltonian of N Fermi oscillators,

$$H = \sum_\kappa \epsilon_\kappa \left(c_\kappa^\dagger c_\kappa - \frac{1}{2} \right),$$
$$\epsilon_\kappa = J\cos\kappa - \mathcal{E}p_0 \sin\kappa - \mathcal{B}m_0$$
$$= \sqrt{J^2 + (\mathcal{E}p_0)^2}\,\cos(\kappa - \varphi) - \mathcal{B}m_0, \qquad (6)$$

$\kappa = 2\pi z/N$, $z = -N/2, -N/2+1, \dots, N/2-1$ ($N \to \infty$ is even) and $\tan\varphi = \mathcal{E}p_0/J$ [17]. The case $\Delta = 1$ results in interacting fermions. Indeed, if $\Delta \neq 0$, the Hamiltonian after fermionization contains the interaction term $\sum_n \Delta(c_n^\dagger c_n - 1/2)(c_{n+1}^\dagger c_{n+1} - 1/2)$; this Hamiltonian can be reduced to free fermions after making a Hartree-Fock approximation [18].

To examine static magnetoelectric effect one has to calculate the magnetic moment $M^z = m_0 \sum_n \langle s_n^z \rangle$ and the electric polarization $P^y = p_0 \sum_n (\langle s_n^x s_{n+1}^y \rangle - \langle s_n^y s_{n+1}^x \rangle)$ for spin model (5); here, $\langle (\dots) \rangle = {\rm Tr}[e^{-H/T}(\dots)]/{\rm Tr}e^{-H/T}$ and H is given in Eq. (6). Since in the fermionic picture $s_n^z = c_n^\dagger c_n - 1/2$ and $s_n^x s_{n+1}^y - s_n^y s_{n+1}^x = {\rm i}(c_n^\dagger c_{n+1} + c_n c_{n+1}^\dagger)/2$, the calculation of the magnetic moment M^z/m_0 or the electric polarization P^y/p_0 reduces to a straightforward application of the Wick theorem.

The ground-state phase diagram of model (5) with $\Delta = 0$ is simple: Until $0 \leq \mathcal{B}m_0 < \sqrt{J^2 + (\mathcal{E}p_0)^2}$ the model is a spin liquid, whereas for

$\mathcal{B}m_0 > \sqrt{J^2 + (\mathcal{E}p_0)^2}$ it is a saturated paramagnet. Such a magnetoelectric crystal shows only a trivial magnetoelectric effect.

In our study on dynamic manifestation of magnetoelectricity, we use microscopic model (5) for calculation of various frequency-dependent susceptibilities, which enter the dispersion relation for the electromagnetic wave propagation, see Section 3. The advantage of the model under consideration is the possibility to calculate the needed dynamic quantities in the fermionic picture rigorously, without making any approximation, see Section 4. Other models would require some (approximate) approach (e.g., Green's functions or numerics) for calculation of dynamic correlations.

3. Electromagnetic wave in magnetoelectric medium

Electromagnetic wave in a medium interacts with the matter of the medium that results, e.g., in the change of the electromagnetic wave speed. Theoretical analysis of the electromagnetic wave propagation in media uses Maxwell's equations in matter, which relate the fields $\boldsymbol{E}$, $\boldsymbol{D}$, $\boldsymbol{B}$, $\boldsymbol{H}$ and free charges ρ and free currents $\boldsymbol{j}$ to each other:

$$\mathrm{div}\boldsymbol{D} = 4\pi\rho, \quad \mathrm{div}\boldsymbol{B} = 0,$$
$$\mathrm{rot}\boldsymbol{E} = -\frac{1}{c}\frac{\partial \boldsymbol{B}}{\partial t}, \quad \mathrm{rot}\boldsymbol{H} = \frac{4\pi}{c}\boldsymbol{j} + \frac{1}{c}\frac{\partial \boldsymbol{D}}{\partial t} \qquad (7)$$

(Gaussian system); besides, these equations must be supplemented by the constitutive relations like $\boldsymbol{D} = \boldsymbol{E} + 4\pi\boldsymbol{P}$, $\boldsymbol{H} = \boldsymbol{B} - 4\pi\boldsymbol{M}$, where the polarization $\boldsymbol{P}$ (electric dipole moment per unit volume) and the magnetization $\boldsymbol{M}$ (magnetic dipole moment per unit volume) describe the material's electric and magnetic response to fields $\boldsymbol{E}$ and $\boldsymbol{H}$. Here, all quantities depend on position $\boldsymbol{r}$ and time t, the Cartesian components of fields are denoted as, e.g., D_α, $\alpha = x, y, z$ and so on. Even though the electromagnetic wave propagation in magnetoelectric medium was studied previously, see, e.g., Ref. [19], we recall these reasonings below keeping in mind the microscopic model of Sec. 2.

Since we consider a monochromatic uniform plane wave that propagates through a nonconducting medium, it is convenient to present any field $\boldsymbol{F}(\boldsymbol{r}, t)$ in a complex form, that is, $\boldsymbol{F}_{\boldsymbol{k}\omega} \exp[{\rm i}(\boldsymbol{k}\cdot\boldsymbol{r} - \omega t)]$, where $\boldsymbol{k}$ is the wave vector and ω is the frequency. After all, the true fields correspond to the real (or imaginary) parts of the complex-form fields. Then

Maxwell's equations (7) supplemented by the constitutive relations read

$$\begin{gathered}\boldsymbol{k}\cdot\boldsymbol{D}_{\boldsymbol{k}\omega}=0,\quad \boldsymbol{k}\cdot\boldsymbol{B}_{\boldsymbol{k}\omega}=0,\\ \boldsymbol{k}\times\boldsymbol{E}_{\boldsymbol{k}\omega}=\frac{\omega}{c}\boldsymbol{B}_{\boldsymbol{k}\omega},\quad \boldsymbol{k}\times\boldsymbol{H}_{\boldsymbol{k}\omega}=-\frac{\omega}{c}\boldsymbol{D}_{\boldsymbol{k}\omega},\\ \boldsymbol{D}_{\boldsymbol{k}\omega}=\boldsymbol{E}_{\boldsymbol{k}\omega}+4\pi\boldsymbol{P}_{\boldsymbol{k}\omega},\quad \boldsymbol{H}_{\boldsymbol{k}\omega}=\boldsymbol{B}_{\boldsymbol{k}\omega}-4\pi\boldsymbol{M}_{\boldsymbol{k}\omega},\end{gathered}\tag{8}$$

and, for a magnetoelectric medium, when the electromagnetic wave interacts weakly with the medium,

$$\begin{aligned}P^{\alpha}_{\boldsymbol{k}\omega}&=\chi^{(\mathrm{ee})}_{\alpha\beta}(\boldsymbol{k},\omega)E^{\beta}_{\boldsymbol{k}\omega}+\chi^{(\mathrm{em})}_{\alpha\beta}(\boldsymbol{k},\omega)H^{\beta}_{\boldsymbol{k}\omega},\\ M^{\alpha}_{\boldsymbol{k}\omega}&=\chi^{(\mathrm{mm})}_{\alpha\beta}(\boldsymbol{k},\omega)H^{\beta}_{\boldsymbol{k}\omega}+\chi^{(\mathrm{me})}_{\alpha\beta}(\boldsymbol{k},\omega)E^{\beta}_{\boldsymbol{k}\omega}.\end{aligned}\tag{9}$$

Bearing in mind the magnetoelectric-crystal model of Sec. 2, we focus on the case when $\boldsymbol{k}=(k^x,0,0)$. Moreover, we consider separately the following two cases:

- $\boldsymbol{E}_{\boldsymbol{k}\omega}=(0,E^y_{\boldsymbol{k}\omega},0)$, $E^y_{\boldsymbol{k}\omega}=E^y$ and $\boldsymbol{B}_{\boldsymbol{k}\omega}=(0,0,B^z_{\boldsymbol{k}\omega})$, $B^z_{\boldsymbol{k}\omega}=B^z$, that is, a plane wave travels along the x (i.e., chain) direction with the electric/magnetic field oscillating along the y/z direction (case 1)

and

- $\boldsymbol{E}_{\boldsymbol{k}\omega}=(0,0,E^z_{\boldsymbol{k}\omega})$, $E^z_{\boldsymbol{k}\omega}=E^z$ and $\boldsymbol{B}_{\boldsymbol{k}\omega}=(0,B^y_{\boldsymbol{k}\omega},0)$, $B^y_{\boldsymbol{k}\omega}=B^y$, that is, a plane wave travels along the x (i.e., chain) direction with the electric/magnetic field oscillating along the z/y direction (case 2).

For the case 1, according to Eq. (8), $E^y=E^y_{\boldsymbol{k}\omega}$ and $H^z=B^z-4\pi M^z$, $B^z=B^z_{\boldsymbol{k}\omega}$ satisfy

$$k^xE^y=\frac{\omega}{c}\left(H^z+4\pi M^z\right),\ k^xH^z=\frac{\omega}{c}\left(E^y+4\pi P^y\right)\tag{10}$$

whereas Eq. (9) reads

$$\begin{aligned}P^y&=\chi^{(\mathrm{ee})}_{yy}E^y+\chi^{(\mathrm{em})}_{yz}H^z,\\ M^z&=\chi^{(\mathrm{mm})}_{zz}H^z+\chi^{(\mathrm{me})}_{zy}E^y,\end{aligned}\tag{11}$$

where we have shortened notations, i.e., $\chi^{(\mathrm{ee})}_{yy}=\chi^{(\mathrm{ee})}_{yy}(k^x,\omega)$ and so on. Combining Eqs. (10) and (11) gives

$$\begin{aligned}k^xE^y&=\frac{\omega}{c}\left[H^z+4\pi\left(\chi^{(\mathrm{mm})}_{zz}H^z+\chi^{(\mathrm{me})}_{zy}E^y\right)\right],\\ k^xH^z&=\frac{\omega}{c}\left[E^y+4\pi\left(\chi^{(\mathrm{ee})}_{yy}E^y+\chi^{(\mathrm{em})}_{yz}H^z\right)\right]\end{aligned}\tag{12}$$

or

$$\begin{gathered}\begin{pmatrix}k^x-4\pi\chi^{(\mathrm{me})}_{zy}\frac{\omega}{c} & -\mu_{zz}\frac{\omega}{c}\\ -\varepsilon_{yy}\frac{\omega}{c} & k^x-4\pi\chi^{(\mathrm{em})}_{yz}\frac{\omega}{c}\end{pmatrix}\begin{pmatrix}E^y\\ H^z\end{pmatrix}=0,\\ \mu_{zz}=1+4\pi\chi^{(\mathrm{mm})}_{zz},\quad \varepsilon_{yy}=1+4\pi\chi^{(\mathrm{ee})}_{yy}.\end{gathered}\tag{13}$$

As a result, one arrives at the equation which determines the dispersion relation $k^x(\omega)$:

$$\frac{ck^x_{\pm}}{2\pi\omega}=\chi^{(\mathrm{me})}_{zy}+\chi^{(\mathrm{em})}_{yz}\pm\sqrt{\frac{\varepsilon_{yy}\mu_{zz}}{4\pi^2}+\left(\chi^{(\mathrm{me})}_{zy}-\chi^{(\mathrm{em})}_{yz}\right)^2}.\tag{14}$$

For the case 2, instead of Eqs. (10) and (11) we have:

$$-k^xE^z=\frac{\omega}{c}\left(H^y+4\pi M^y\right),\ k^xH^y=-\frac{\omega}{c}\left(E^z+4\pi P^z\right)\tag{15}$$

and

$$\begin{aligned}P^z&=\chi^{(\mathrm{ee})}_{zz}E^z+\chi^{(\mathrm{em})}_{zy}H^y,\\ M^y&=\chi^{(\mathrm{mm})}_{yy}H^y+\chi^{(\mathrm{me})}_{yz}E^z.\end{aligned}\tag{16}$$

Now, combining Eqs. (15) and (16) gives

$$\begin{aligned}-k^xE^z&=\frac{\omega}{c}\left[H^y+4\pi\left(\chi^{(\mathrm{mm})}_{yy}H^y+\chi^{(\mathrm{me})}_{yz}E^z\right)\right],\\ k^xH^y&=-\frac{\omega}{c}\left[E^z+4\pi\left(\chi^{(\mathrm{ee})}_{zz}E^z+\chi^{(\mathrm{em})}_{zy}H^y\right)\right]\end{aligned}\tag{17}$$

or

$$\begin{gathered}\begin{pmatrix}-k^x-4\pi\chi^{(\mathrm{me})}_{yz}\frac{\omega}{c} & -\mu_{yy}\frac{\omega}{c}\\ \varepsilon_{zz}\frac{\omega}{c} & k^x+4\pi\chi^{(\mathrm{em})}_{zy}\frac{\omega}{c}\end{pmatrix}\begin{pmatrix}E^z\\ H^y\end{pmatrix}=0,\\ \mu_{yy}=1+4\pi\chi^{(\mathrm{mm})}_{yy},\quad \varepsilon_{zz}=1+4\pi\chi^{(\mathrm{ee})}_{zz}.\end{gathered}\tag{18}$$

As a result, one arrives at the equation which determines the dispersion relation $k^x(\omega)$:

$$\frac{ck^x_{\pm}}{2\pi\omega}=-\left(\chi^{(\mathrm{me})}_{yz}+\chi^{(\mathrm{em})}_{zy}\right)\pm\sqrt{\frac{\varepsilon_{zz}\mu_{yy}}{4\pi^2}+\left(\chi^{(\mathrm{me})}_{yz}-\chi^{(\mathrm{em})}_{zy}\right)^2},\tag{19}$$

cf. Eq. (14).

Note that $k^x_{\pm}(\omega)$ in the dispersion relation is, generally speaking, a complex function, i.e., $k^x_{\pm}(\omega)=k'_{\pm}(\omega)+\mathrm{i}k''_{\pm}(\omega)$. The real part $k'_{\pm}(\omega)$

yields the wave's phase velocity $v_\omega = \omega/k'_\pm(\omega)$ while the imaginary part $k''_\pm(\omega) > 0$ forms the attenuation coefficient. Besides, the ratio between the speed of light c and the phase velocity v_ω is known as the (real part of) refractive index, $n_\omega = c/v_\omega$. (The refractive index is also a complex-valued function of ω: $n' + \mathrm{i}n'' = c(k' + \mathrm{i}k'')/\omega$.)

For $\chi^{(\mathrm{me})}_{zy} = \chi^{(\mathrm{em})}_{yz} = 0$, Eq. (14) yields the well-known result: $k^x_\pm(\omega) = \pm\omega\sqrt{\varepsilon_{yy}\mu_{zz}}/c$. Similarly, for $\chi^{(\mathrm{me})}_{yz} = \chi^{(\mathrm{em})}_{zy} = 0$, Eq. (19) yields $k^x_\pm(\omega) = \pm\omega\sqrt{\varepsilon_{zz}\mu_{yy}}/c$. Obviously, the velocity for traveling forward and backward is the same.

In contrast, in a magnetoelectric medium, when $\chi^{(\mathrm{me})}_{zy} \neq 0$, $\chi^{(\mathrm{em})}_{yz} \neq 0$ (Eq. (14)) or $\chi^{(\mathrm{me})}_{yz} \neq 0$, $\chi^{(\mathrm{em})}_{zy} \neq 0$ (Eq. (19)), these velocities become different:

$$\frac{\omega}{k^x_\pm} = f^{(14)}_\pm \frac{c}{\sqrt{\varepsilon_{yy}\mu_{zz}}},$$
$$\frac{1}{f^{(14)}_\pm} = \pm\sqrt{1 + \frac{4\pi^2\left(\chi^{(\mathrm{me})}_{zy} - \chi^{(\mathrm{em})}_{yz}\right)^2}{\varepsilon_{yy}\mu_{zz}}} + \frac{2\pi\left(\chi^{(\mathrm{me})}_{zy} + \chi^{(\mathrm{em})}_{yz}\right)}{\sqrt{\varepsilon_{yy}\mu_{zz}}};$$
$$\frac{\omega}{k^x_\pm} = f^{(19)}_\pm \frac{c}{\sqrt{\varepsilon_{zz}\mu_{yy}}},$$
$$\frac{1}{f^{(19)}_\pm} = \pm\sqrt{1 + \frac{4\pi^2\left(\chi^{(\mathrm{me})}_{yz} - \chi^{(\mathrm{em})}_{zy}\right)^2}{\varepsilon_{zz}\mu_{yy}}} - \frac{2\pi\left(\chi^{(\mathrm{me})}_{yz} + \chi^{(\mathrm{em})}_{zy}\right)}{\sqrt{\varepsilon_{zz}\mu_{yy}}}; \qquad (20)$$

i.e., the propagation velocity is modified by the factor $f_\pm$ which deviates from ± 1 and leads to a directional nonreciprocity, that is, a difference in the electromagnetic wave propagation between opposite directions.

At the end, let us consider the limiting case of the spin-1/2 isotropic XY chain in a transverse field, when there is no the contribution from the electric polarization of the bond in Eq. (5), i.e., $p_0 = 0$. In this limit only magnetic component of the electromagnetic wave weakly interacts with the quantum spin chain. For the case 1, $k^x_\pm(\omega) = \pm\omega\sqrt{1 + 4\pi(\chi'_{zz} + \mathrm{i}\chi''_{zz})}/c$, where $\chi^{(\mathrm{mm})}_{zz} = \chi'_{zz} + \mathrm{i}\chi''_{zz}$ and the values of χ'_{zz} and χ''_{zz} are taken at the frequency ω and $\kappa = 0$. By symmetry, $\chi^{(\mathrm{mm})}_{zz} = 0$ at $\kappa = 0$ (see Sec. 4). For the case 2, $k^x_\pm(\omega) = \pm\omega\sqrt{1 + 4\pi(\chi'_{yy} + \mathrm{i}\chi''_{yy})}/c$, where $\chi^{(\mathrm{mm})}_{yy} = \chi'_{yy} + \mathrm{i}\chi''_{yy}$ and the values of χ'_{yy} and χ''_{yy} are taken at the frequency ω and $\kappa = 0$. Now, however, $\chi^{(\mathrm{mm})}_{yy} \neq 0$ at $\kappa = 0$ and it depends on the frequency ω.

To summarize this section, electromagnetic wave propagation in a magnetoelectric medium has been examined within the frames of the classical electrodynamics of a continuous medium and it promises to exhibit interesting features. The dispersion relation involves the dynamic (i.e., frequency-dependent) susceptibilities for a quantum spin chain which constitutes the magnetoelectric medium under consideration. Therefore, we turn now to calculation of dynamic susceptibilities for a free-fermion quantum spin chain.

4. Dynamic susceptibilities

To proceed the analysis of propagation of the plane electromagnetic wave in the magnetoelectric crystal, defined in Sec. 2, we need the susceptibilities $\chi^{(\mathrm{mm})}_{zz}(\kappa,\omega)$, $\chi^{(\mathrm{mm})}_{yy}(\kappa,\omega)$, $\chi^{(\mathrm{ee})}_{yy}(\kappa,\omega)$, $\chi^{(\mathrm{ee})}_{zz}(\kappa,\omega)$, $\chi^{(\mathrm{me})}_{zy}(\kappa,\omega)$, $\chi^{(\mathrm{me})}_{yz}(\kappa,\omega)$, $\chi^{(\mathrm{em})}_{yz}(\kappa,\omega)$, and $\chi^{(\mathrm{em})}_{zy}(\kappa,\omega)$, defined in Eq. (9). After all, they determine the forward/backward propagation according to Eqs. (14), (19), and (20). On the other hand, we can calculate the dimensionless (i.e., ignoring the unknown p_0 and m_0) susceptibilities $\chi^{(\mathrm{ab})}_{\alpha\beta}(\kappa,\omega)$ for the quantum spin model (5), see below, which should be proportional to the ones defined in Eq. (9). Bearing in mind the inspection of frequency dependencies, we set for simplicity the constant of proportionality to 1. As a consequence, we will illustrate how the electromagnetic-wave propagation can be controlled by varying the parameters $\mathcal{E}$ or $\mathcal{B}$ in Eq. (5) (and also J' if more complicated Hamiltonian is considered).

More specifically, according to the linear response theory,

$$\chi_{AB}(t_2 - t_1) = \frac{\mathrm{i}}{\hbar}\theta(t_2 - t_1)\langle[A(t_2), B(t_1)]\rangle_0 \qquad (21)$$

(Kubo formula), and $\chi_{AB}(t_2 - t_1)$ is directly related to a double-time Green's function,

$$G^{\mathrm{retarded}}_{AB}(t_2, t_1) = -\mathrm{i}\theta(t_2 - t_1)\langle[A(t_2), B(t_1)]\rangle, \qquad (22)$$

see, e.g., [20]. In our study, we consider for A and B the following local operators:

$$\frac{p^y_{n,n+1}}{p_0} = s^x_n s^y_{n+1} - s^y_n s^x_{n+1} = \frac{\mathrm{i}}{2}\left(c^\dagger_n c_{n+1} + c_n c^\dagger_{n+1}\right),$$
$$\frac{p^z_{n,n+1}}{p_0} = s^x_n s^z_{n+1} - s^z_n s^x_{n+1}$$
$$= \prod_{j=1}^{n-1}\left(1 - 2c^\dagger_j c_j\right)\frac{c^\dagger_n + c_n}{2}\left(c^\dagger_{n+1} c_{n+1} - \frac{1}{2}\right)$$

$$-\left(c_n^\dagger c_n-\frac{1}{2}\right)\prod_{j=1}^{n}\left(1-2c_j^\dagger c_j\right)\frac{c_{n+1}^\dagger+c_{n+1}}{2},$$

$$\frac{m_n^y}{m_0}=\frac{s_n^+-s_n^-}{2\mathrm{i}}=\prod_{j=1}^{n-1}\left(1-2c_j^\dagger c_j\right)\frac{c_n^\dagger-c_n}{2\mathrm{i}},$$

$$\frac{m_n^z}{m_0}=s_n^+s_n^--\frac{1}{2}=c_n^\dagger c_n-\frac{1}{2}, \tag{23}$$

and calculate dynamic (frequency-dependent) susceptibilities like

$$\chi_{zz}^{(\mathrm{mm})}(\kappa,\omega)=\frac{1}{m_0^2}\sum_{n=1}^{N}e^{\mathrm{i}\kappa n}\int_0^\infty \mathrm{d}t e^{\mathrm{i}\omega t}\mathrm{i}\langle\left[m_j^z(t),m_{j+n}^z\right]\rangle, \tag{24}$$

and so on at $\kappa=0$. In what follows, the unknown factors m_0 and p_0 have dropped out. Some of these susceptibilities are governed by two-fermion continua and it is possible to examine them in great detail, see Ref. [21]. The other ones are governed by many-fermion continua and it is possible to examine them in great detail numerically, see Refs. [21–23].

Postponing consideration of a quantum chain with KNB mechanism for a full paper, in this preliminary notes we focus on the *antiferromagnetic* chain without KNB mechanism, i.e., $p_0=0$ in Eq. (5). (The results for the *ferromagnetic* chain without KNB mechanism are reported in Appendix B.) Thus, Eq. (14) reads: $ck_\pm^x/\omega=\pm\sqrt{1+4\pi\chi_{zz}}$, and Eq. (19) reads: $ck_\pm^x/\omega=\pm\sqrt{1+4\pi\chi_{yy}}$. Moreover, the two-fermion quantity $\chi_{zz}(\kappa=0,\omega)=0$ (recall that $[\sum_{n=1}^N s_n^z,H]=0$). In contrast, the many-fermion quantity $\chi_{yy}(\kappa,\omega)=\chi_{xx}(\kappa,\omega)$ may be nonzero at $\kappa=0$. Therefore, for the spin-1/2 isotropic XY chain in a transverse field in case 1 the dispersion relation remains as in vacuum, but in case 2 it becomes

$$\frac{ck(\omega)}{\omega}=\sqrt{1+4\pi\left(\chi_{xx}'(0,\omega)+\mathrm{i}\chi_{xx}''(0,\omega)\right)}$$

$$=\sqrt{\sqrt{\left(1+4\pi\chi_{xx}'(0,\omega)\right)^2+\left(4\pi\chi_{xx}''(0,\omega)\right)^2}e^{\mathrm{i}\frac{\alpha}{2}}},$$

$$\tan\alpha=\frac{4\pi\chi_{xx}''(0,\omega)}{1+4\pi\chi_{xx}'(0,\omega)}, \tag{25}$$

where $k_\pm^x=\pm k(\omega)$. Clearly, $ck'(\omega)/\omega\geq 1$ means that the wave's phase velocity does not exceed c. (The phase velocity can be greater than c; this is not a violation of special relativity. However, the group velocity should be always less than or equal to c.)

We calculate $\chi_{xx}(\kappa,\omega)$ in Eq. (25) numerically following the lines of Refs. [21–23] (for more recent study see [24]) and report our findings in Fig. 1. In our calculations, we take $N=1600$, $j=301$, calculate correlations up to $n=100$, and integrate over time (see Eq. (24)) till $t=100$ (for structure factor (26) from -100 to 100). We also introduce a small damping parameter changing the real ω to $\omega+\mathrm{i}\varepsilon$ with $\varepsilon=0$ (small $\mathcal{B}<1$) or $\varepsilon=0.05$ (large $\mathcal{B}\geq 1$). In addition, instead of zero temperature we consider sufficiently low one $T=0.02$. Our findings are reported in Fig. 1. Furthermore, we insert $\chi_{xx}(\kappa=0,\omega)$ into Eq. (25) to obtain $k(\omega)=k'(\omega)+\mathrm{i}k''(\omega)$ presented in Fig. 2. We discuss these results in the next section.

In addition, we calculate the dynamic structure factor

$$S_{xx}(0,\omega)=\sum_{n=1}^{N}e^{\mathrm{i}\kappa n}\int_{-\infty}^{\infty}\mathrm{d}t e^{-\varepsilon|t|}e^{\mathrm{i}\omega t}\langle s_j^x(t)s_{j+n}\rangle$$

$$=\frac{2}{1-e^{-\frac{\omega}{T}}}\Im\chi_{xx}(0,\omega). \tag{26}$$

The latter relation gives $\Im\chi_{xx}(0,\omega)$ also for $\omega<0$, because $\Im\chi_{xx}(0,\omega)$ is antisymmetric with respect to ω. Furthermore, $\Re\chi_{xx}(0,\omega)$ follows from the Kramers-Kronig relations,

$$\Re\chi_{xx}(0,\omega)=\frac{1}{\pi}\mathcal{P}\int_{-\infty}^{\infty}\mathrm{d}\omega'\frac{\Im\chi_{xx}(\omega')}{\omega'-\omega},$$

$$\Im\chi_{xx}(0,\omega)=-\frac{1}{\pi}\mathcal{P}\int_{-\infty}^{\infty}\mathrm{d}\omega'\frac{\Re\chi_{xx}(\omega')}{\omega'-\omega}, \tag{27}$$

$\mathcal{P}$ denotes the Cauchy principal value, for $\chi_{xx}(0,\omega)=\Re\chi_{xx}(0,\omega)+\mathrm{i}\Im\chi_{xx}(0,\omega)$. In Fig. 3 we illustrate the consistency (i) of direct calculation of $\chi_{xx}(0,\omega)$ and (ii) of calculation of $\chi_{xx}(0,\omega)$ through $S_{xx}(0,\omega)$ with using Eqs. (26) and (27).

It is worthy to recall here that in the strong-field and zero-temperature limit the time-dependent correlation functions $\langle s_j^x(t)s_{j+n}^x\rangle$ can be calculated rigorously [25–28]. Namely, for model (5) with $\Delta=0$, $p_0=0$, and $m_0=1$ we have

$$\langle s_j^x(t)s_{j+n}^x(0)\rangle=\frac{1}{8\pi}\int_{-\pi}^{\pi}\mathrm{d}\kappa e^{\mathrm{i}\kappa n-\mathrm{i}\epsilon_\kappa t},$$

$$\epsilon_\kappa=J\cos\kappa-\mathcal{B}. \tag{28}$$

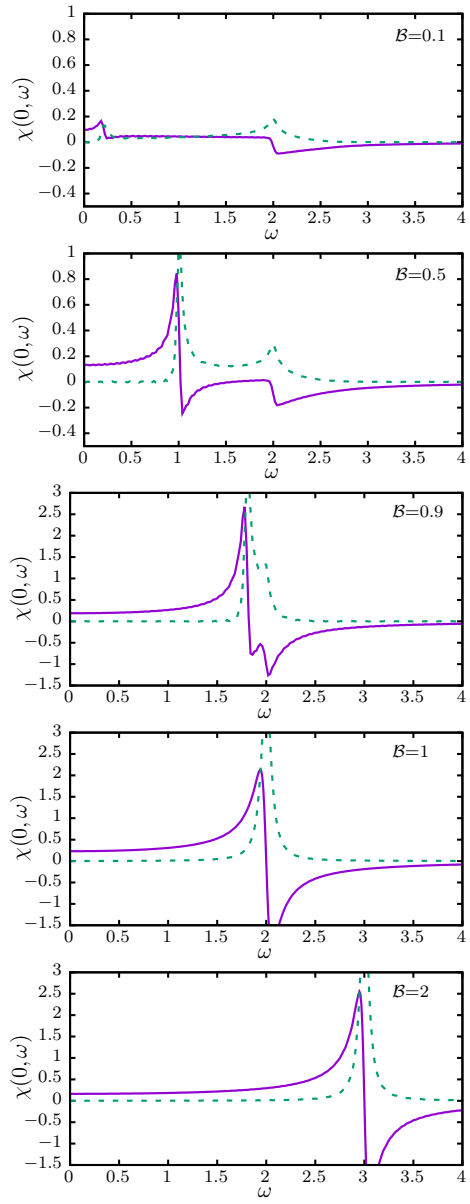

Figure 1. $\chi'_{xx}(\kappa=0,\omega)$ (solid) and $\chi''_{xx}(\kappa=0,\omega)$ (dashed) for the spin-1/2 isotropic XY antiferromagnetic chain in a transverse field ($J=1$, $p_0=0$, $J'=0$). $T=0.02$.

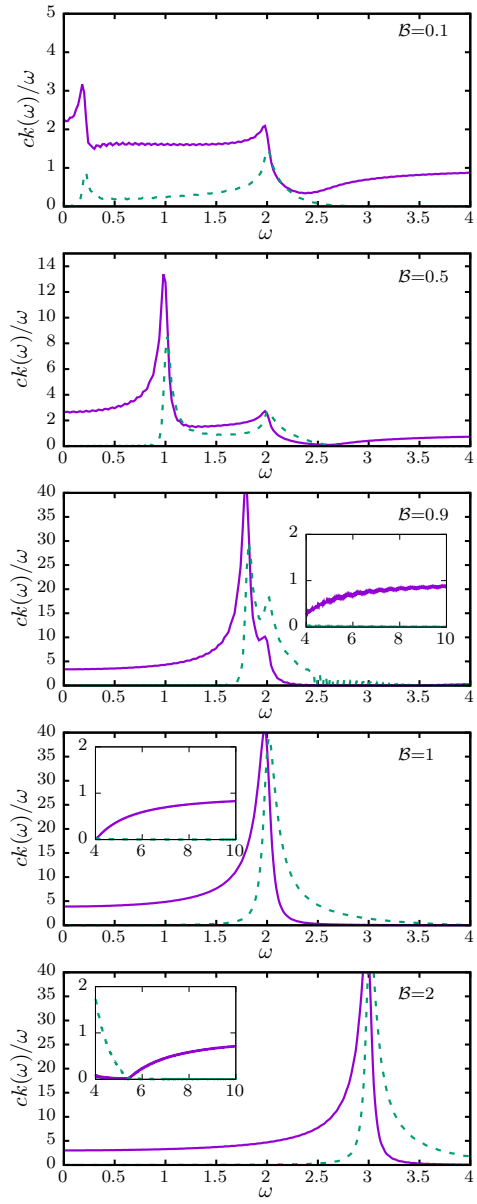

Figure 2. Towards the dispersion relation $k(\omega)$: $ck'(\omega)/\omega$ (solid) and $ck''(\omega)/\omega$ (dashed) for the spin-1/2 isotropic XY antiferromagnetic chain in a transverse field ($J=1$, $p_0=0$, $J'=0$). $T=0.02$.

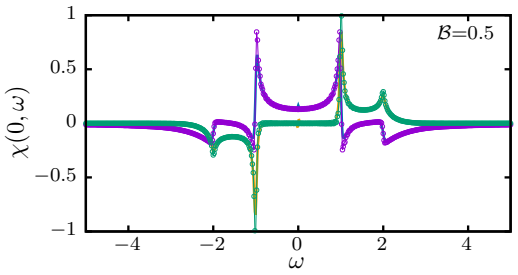

Figure 3. $\Re\chi_{xx}(0,\omega)$ and $\Im\chi_{xx}(0,\omega)$ ($J=1$, $\mathcal{B}=0.5$, $T=0.02$): Direct calculation according definition similar to Eq. (24) versus calculation of $S_{xx}(0,\omega)$ (26) and then using Eqs. (26) and (27).

As a result, we immediately obtain $\chi_{xx}(0,\omega)$ following the definition, cf. Eq. (24). The results are shown in Fig. 4 ($\varepsilon=0.05$); they are indistinguishable from the ones obtained by numerical calculation at $T=0.02$.

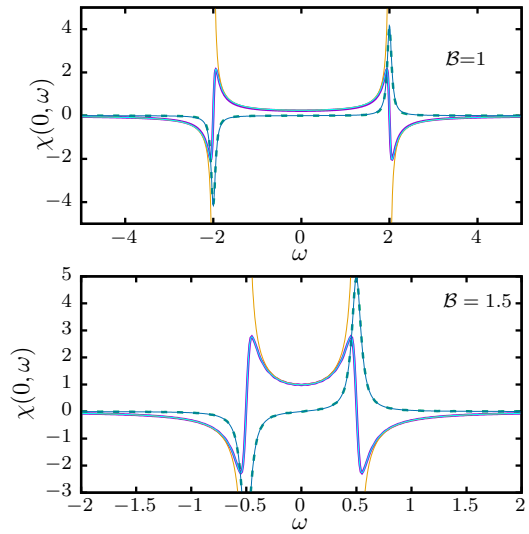

Figure 4. Strong-field low-temperature regime: Numerical calculation of $\Re\chi_{xx}(0,\omega)$ and $\Im\chi_{xx}(0,\omega)$ ($T=0.02$, $\varepsilon=0.05$) and as they follow from Eq. (28) ($\varepsilon=0.05$); both results are hardly distinguishable. Besides, we show the Landau-Lifshitz-equation prediction (32) (golden curves). (Top) $J=1$, $\mathcal{B}=1$. (Bottom) $J=-1$, $\mathcal{B}=1.5$.

Interestingly, the strong-field zero-temperature limit case can be understood from a completely different perspective, that is, using the Landau-Lifshitz equation, which describes the magnetization vector in ferromagnetic material. Thus, the equation of motion for the magnetization $\boldsymbol{M}$ reads

$$\frac{\mathrm{d}\boldsymbol{M}}{\mathrm{d}t}=\gamma\left[(\mathbf{H}+\beta M_z\boldsymbol{\nu})\times\boldsymbol{M}\right], \tag{29}$$

where $\gamma=g|e|/2mc$ (g being the gyromagnetic ratio), $\beta>0$ is the anisotropy coefficient, and $\boldsymbol{\nu}$ is the unit vector along the axis of easy magnetization (the z-axis), see Ref. [29], page 270, problem 1. Next, $\boldsymbol{H}=\boldsymbol{H}_0+\boldsymbol{H}'$, where $\boldsymbol{H}_0$ is a constant field along the z-axis and $\boldsymbol{H}'$ is a small alternating field in any direction. Clearly, $M_z\approx M$, whereas the transverse magnetization M_x and M_y are small. Neglecting small quantities, Eq. (29) can be cast into

$$\begin{aligned}-\mathrm{i}\omega M_x&=-\gamma\left(H_0+\beta M\right)M_y+\gamma M H'_y,\\ -\mathrm{i}\omega M_y&=\gamma\left(H_0+\beta M\right)M_x-\gamma M H'_x.\end{aligned} \tag{30}$$

Determining now M_x and M_y, we find the susceptibility and hence the permeability:

$$\begin{aligned}\mu_{xx}=\mu_{yy}&=1-\frac{4\pi}{\beta}\frac{\omega_M\left(\omega_M+\omega_H\right)}{\omega^2-\left(\omega_M+\omega_H\right)^2},\ \mu_{zz}=1,\\ \mu_{xy}=-\mu_{yx}&=\mathrm{i}\frac{4\pi}{\beta}\frac{\omega\omega_M}{\omega^2-\left(\omega_M+\omega_H\right)^2},\ \mu_{xz}=\mu_{yz}=0,\end{aligned} \tag{31}$$

where $\omega_M=\gamma\beta M$ and $\omega_H=\gamma H_0$, see Ref. [29], page 270, problem 1. Making change $\omega_M\to\beta/2$ and $\omega_M+\omega_H\to J+\mathcal{B}$, we obtain

$$\chi_{xx}(0,\omega)=-\frac{1}{2}\frac{J+\mathcal{B}}{\omega^2-\left(J+\mathcal{B}\right)^2}, \tag{32}$$

which is shown by golden curves in Fig. 4 for $J=1$, $\mathcal{B}=1$ (top panel) and $J=-1$, $\mathcal{B}=1.5$ (bottom panel).

5. Results and outlook

Let us discuss the electromagnetic wave propagation through the magnetoelectric medium consisting of noninteracting KNB chains, each of which with the Hamiltonian given in Eq. (5), $\Delta=0$, as it follows from

the analysis of Secs. 3 and 4. Recall that meanwhile we have set $p_0 = 0$, i.e., switched off the KNB mechanism.

There are two parameters in the problem: ω/J (electromagnetic wave frequency) and $\mathcal{B}/J$ (magnetic field magnitude). In the high-frequency limit $\omega/J \gg 1$, as can be seen in Fig. 2, $ck'/\omega \to 1$, $ck''/\omega \to 0$ (also for $\mathcal{B} = 0.9$, 1, 2, see the insets in Fig. 2) that indicates electromagnetic wave propagation as in vacuum (electromagnetic wave of high frequency does not notice the quantum spin chain). In the opposite low-frequency limit $\omega/J \ll 1$, as can be seen in Fig. 2, $ck'/\omega > ck''/\omega \to 0$ that illustrates again no attenuation of the electromagnetic wave.

More complicated picture emerges at intermediate values of ω/J (terahertz frequency range) when attenuation shows up (dashed curves in Fig. 2). Moreover, the value of $\mathcal{B}/J$ is important, too. In the case of strong field $\mathcal{B}/J \geq 1$, one observes a diminishing of the electromagnetic wave velocity accompanied by damping at $\omega = J + \mathcal{B}$, see the panels for $\mathcal{B} = 2$, 1 in Fig. 2. (This is in accordance with the behavior of $\chi(0, \omega)$ shown in Fig. 1.) Such a behavior of medium may resemble a noninteracting spin 1/2, which adsorbs the electromagnetic-wave energy ($\mathcal{B}$ is perpendicular to XY plane, antiferromagnetic interaction between neighboring spins J is in XY plane, magnetic component of electromagnetic wave oscillates along y axis). The case of weak field $\mathcal{B}/J < 1$ is even more intricate, see the panels for $\mathcal{B} = 0.9$, 0.5, 0.1 in Fig. 2. Namely, according to these plots, there are two characteristic frequencies, $\omega_2 = 2$ and $\omega_1 = 2\mathcal{B}$. In the frequency range between ω_1 and ω_2, for $\mathcal{B} = 0.1$ and $\mathcal{B} = 0.5$, $ck'(\omega)/\omega > ck''(\omega)/\omega$, both quantities are comparable that implies a propagation with reduced velocity and some damping. For $\mathcal{B} = 0.9$, ω_1 almost approaches ω_2 and the picture resembles qualitatively the ones for $\mathcal{B} = 1$, cf. the corresponding panels in Fig. 2. Obviously, by varying $\mathcal{B}$, one can control a spreading of electromagnetic wave through the media under consideration.

To summarize, we present a rigorous analysis of electromagnetic wave propagation through electromagnetic media which is based on macroscopic electrodynamics and microscopic calculation of relevant dynamic susceptibilities for a free-fermion KNB quantum spin chain. Although in the present preliminary notes we report the results for the chain without KNB mechanism, a generalization for the case with KNB mechanism is straightforward. We focus on the antiferromagnetic sign of interspin interaction, although the ferromagnetic sign of interspin interaction can be easily considered, too (see Appendix B). Among specific features of the utilized quantum spin model is a spin liquid phase at $T = 0$ until $\mathcal{B}m_0$ does not exceed J and a saturated paramagnetic phase if $\mathcal{B}m_0$ exceeds J. Switching on the KNB mechanism leads to the directional nonreciprocity implying a difference in the electromagnetic wave propagation between opposite directions along the chain. This feature may be related to a diode effect, when magnetoelectric system allows terahertz electromagnetic wave to propagate only in one direction (in analogy to the nonreciprocal resistive charge transport in semiconducting diode). From solid-state point of view, our analysis may be useful as a guide while considering more realistic models which are not exactly solvable. Finally, although in this study we discuss dynamic magnetoelectric effect for electromagnetic wave propagation, other dynamic properties of magnetoelectrics are of interest, too.

Data availability statement

The data that support the findings of this study are available from the authors upon reasonable request.

Acknowledgements

The authors are thankful to the Armed Forces of Ukraine for protection since 2014, and especially since February 24, 2022. This study got funding within the IEEE program Magnetism for Ukraine 2025, supported by the IEEE Magnetic Society under the Science and Technology Center in Ukraine framework; project title: Dynamic properties of one-dimensional magnetoelectric crystal. The authors thank the participants of the seminar of the ICMP Department for Quantum Statistics (December 9, 2025) for discussions.

Appendix A: Three-spin interactions. Two-fermion dynamic structure factor

To illustrate the ground-state phases of model (5) with the three-spin $XZY - YZX$ interaction [30], let us consider three representative values of the latter interaction: $J' = 0$, $J' = 0.5$, and $J' = 0.9$. As is shown in Fig. 5, the model (5) with J' exhibits three ground-state phases, which correspond to different numbers of Fermi points κ^*, which satisfy the equation $\epsilon_{\kappa^*} = 0$, see Eq. (6). Namely, the saturated paramagnet phase (no Fermi points), the spin-liquid I phase (two Fermi points), and the spin-liquid II phase (four Fermi points). For extensive discussion of magnetization and polarization on magnetic/electric field see Ref. [11].

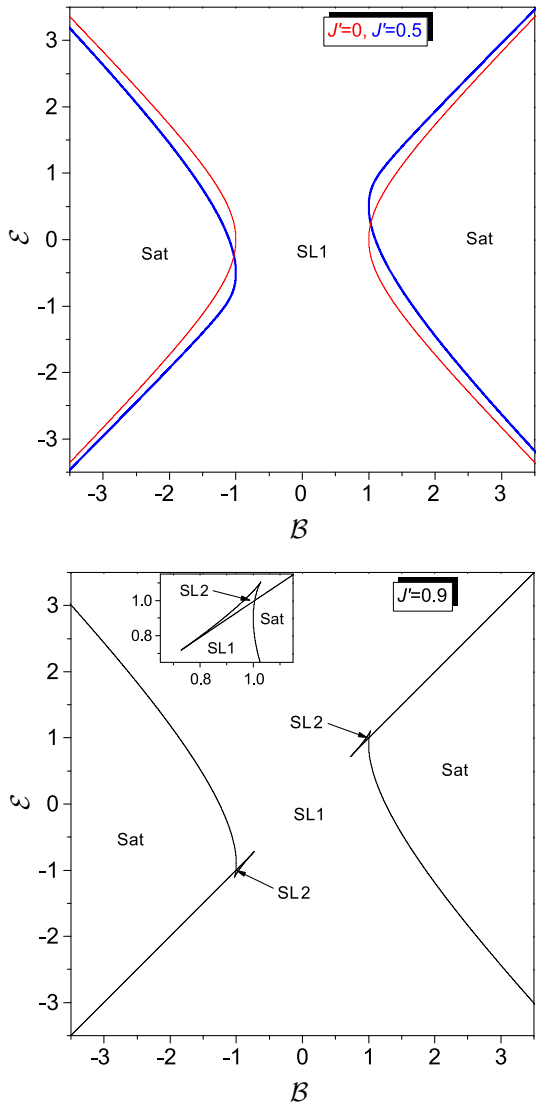

Figure 5. Ground-state phase diagram of model (5) ($J = 1$, $\Delta = 0$, $p_0 = m_0 = 1$) with the $XZY - YZX$ interaction J' in the plane $\mathcal{B} - \mathcal{E}$. Top: $J' = 0$ (red) and $J' = 0.5$ (blue). Bottom: $J' = 0.9$.

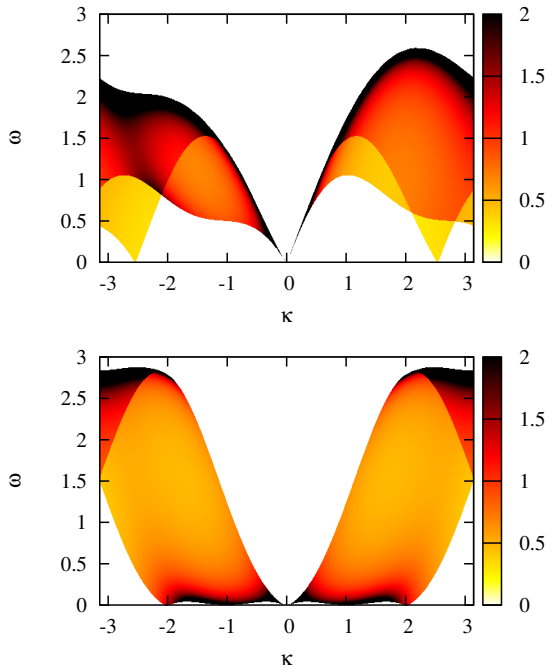

Figure 6. Ground-state structure factor $S_{zz}(\kappa, \omega)$ (A.1) for model (5) with $J = 1$, $\Delta = 0$, $p_0 = m_0 = 1$, and $J' = 0.9$. Top: $\mathcal{B} = 0$ and $\mathcal{E} = 0.5$. Bottom: $\mathcal{B} = 0.95$ and $\mathcal{E} = 1$.

In Fig. 6 we present the zz dynamic structure factor,

$$S_{zz}(\kappa, \omega) = \sum_{n=1}^{N} e^{\mathrm{i}\kappa n} \int_{-\infty}^{\infty} \mathrm{d}t e^{-\varepsilon|t|} e^{\mathrm{i}\omega t} \langle s_j^z(t) s_{j+n}^z \rangle \propto \Im \chi_{zz}^{(\mathrm{mm})}(\kappa, \omega), \tag{A.1}$$

which is governed exclusively by two-fermion continua. For more details about the properties of two-fermion excitation continua see [27, 28].

Appendix B: Ferromagnetic chain

In this appendix, we report our findings for $\chi_{xx}(0, \omega) = \chi'_{xx}(0, \omega) + \mathrm{i}\chi''_{xx}(0, \omega)$ and $k(\omega)$ for the case $J = -|J| < 0$ (and $\Delta = 0$, $p_0 = 0$) in Eq. (5), see Fig. 7 and Fig. 8, respectively. In comparison to Figs. 1 and

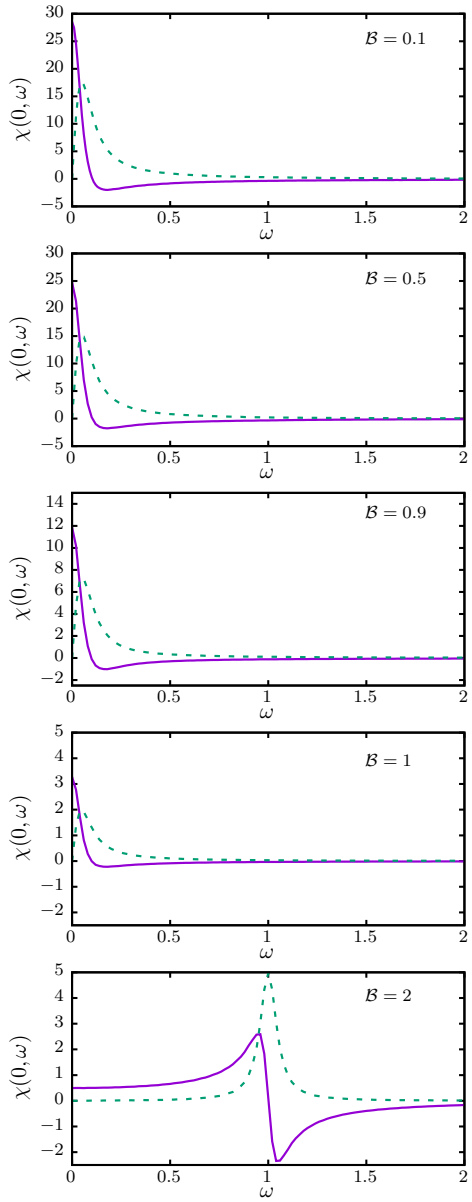

Figure 7. $\chi'_{xx}(\kappa = 0, \omega)$ (solid) and $\chi''_{xx}(\kappa = 0, \omega)$ (dashed) for the spin-1/2 isotropic XY ferromagnetic chain in a transverse field ($J = -1$, $p_0 = 0$, $J' = 0$). $T = 0.02$.

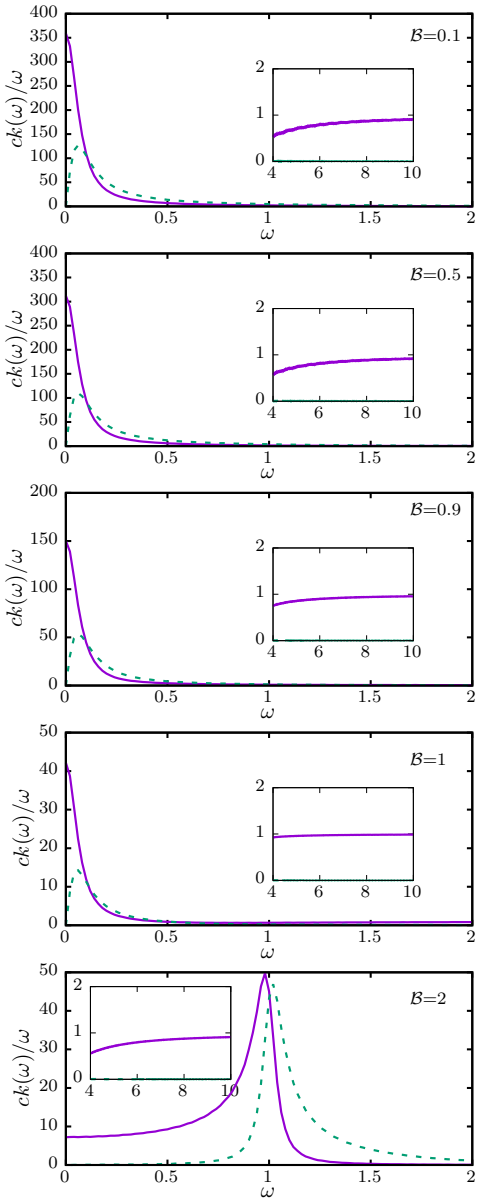

Figure 8. Towards the dispersion relation $k(\omega)$: $ck'(\omega)/\omega$ (solid) and $ck''(\omega)/\omega$ (dashed) for the spin-1/2 isotropic XY ferromagnetic chain in a transverse field ($J = -1$, $p_0 = 0$, $J' = 0$). $T = 0.02$.

2, the results are less spectacular. In the high-frequency limit $\omega/|J| \gg 1$, $ck'/\omega \to 1$ and $ck''/\omega \to 0$, see the insets in Fig. 8. In the low-frequency limit $\omega/|J| \ll 1$, $ck'/\omega \gg ck''/\omega \to 0$. Besides, until $\mathcal{B} \leq |J|$, ck'/ω has maximum at $\omega = 0$ and ck''/ω has maximum slightly above $\omega = 0$. As $\mathcal{B}/|J| > 1$, a new feature appears at intermediate values of ω/J: Then, both frequency dependencies, $ck'(\omega)/\omega$ and $ck''(\omega)/\omega$, exhibit peaks roughly at $\omega = \mathcal{B} - |J|$. In summary, the ferromagnetic case is less suitable for manipulation of electromagnetic wave spreading by varying $\mathcal{B}$.

References

1. H. Katsura, N. Nagaosa, and A. V. Balatsky, Phys. Rev. Lett. **95**, 057205 (2005).
2. P. Fazekas, *Lecture Notes on Electron Correlation and Magnetism* (World Scientific, 1999).
3. S. Miyahara and N. Furukawa, Phys. Rev. B **93**, 014445 (2016).
4. A. Bolens, H. Katsura, M. Ogata, and S. Miyashita, Phys. Rev. B **97**, 161108 (2018).
5. A. Bolens, Phys. Rev. B **98**, 125135 (2018).
6. R. Chari, R. Moessner, and J. G. Rau, Phys. Rev. B **103**, 134444 (2021).
7. S. C. Furuya and M. Sato, Phys. Rev. Res. **6**, 013228 (2024).
8. I. V. Solovyev, Condensed Matter **10** (2025).
9. M. Brockmann, A. Klümper, and V. Ohanyan, Phys. Rev. B **87**, 054407 (2013).
10. W. Brenig, Two-dimensional nonlinear dynamical response of the magnetoelectrically driven dimerized spin-1/2 chain (2025), arXiv:2507.17823 [cond-mat.str-el] .
11. O. Menchyshyn, V. Ohanyan, T. Verkholyak, T. Krokhmalskii, and O. Derzhko, Phys. Rev. B **92**, 184427 (2015).
12. J. Sznajd, Phys. Rev. B **97**, 214410 (2018).
13. O. Baran, V. Ohanyan, and T. Verkholyak, Phys. Rev. B **98**, 064415 (2018).
14. J. Strečka, L. Gálisová, and T. Verkholyak, Phys. Rev. E **101**, 012103 (2020).
15. J. Richter, V. Ohanyan, J. Schulenburg, and J. Schnack, Phys. Rev. B **105**, 054420 (2022).
16. E. Lieb, T. Schultz, and D. Mattis, Annals of Physics **16**, 407 (1961).
17. O. Derzhko, J. Richter, and O. Zaburannyi, Journal of Physics: Condensed Matter **12**, 8661 (2000).

18. S. Yamamoto and K. Funase, Low Temperature Physics **31**, 740 (2005).
19. R. R. Birss and R. G. Shrubsall, The Philosophical Magazine: A Journal of Theoretical Experimental and Applied Physics **15**, 687 (1967).
20. D. N. Zubarev, Soviet Physics Uspekhi **3**, 320 (1960).
21. T. Krokhmalskii, O. Derzhko, J. Stolze, and T. Verkholyak, Phys. Rev. B **77**, 174404 (2008).
22. O. Derzhko and T. Krokhmalskii, Phys. Rev. B **56**, 11659 (1997).
23. O. Derzhko and T. Krokhmalskii, physica status solidi (b) **208**, 221 (1998).
24. U. E. Khodaeva, D. L. Kovrizhin, and J. Knolle, Phys. Rev. B **113**, 045120 (2026).
25. H. B. Cruz and L. L. Goncalves, Journal of Physics C: Solid State Physics **14**, 2785 (1981).
26. O. Derzhko, T. Krokhmalskii, and J. Stolze, Journal of Physics A: Mathematical and General **35**, 3573 (2002).
27. J. Jędrzejewski, *Condensed Matter Physics in the Prime of the 21st Century* (World Scientific, 2008).
28. O. Derzhko, Jordan-Wigner Fermionization and the Theory of Low-Dimensional Quantum Spin Models. Dynamic Properties, in *Condensed Matter Physics in the Prime of the 21st Century*, pp. 35–87.
29. L. Landau and E. Lifshitz, *Electrodynamics of Continuous Media*, Volume 8 of Course of Theoretical Physics (Pergamon Press, 1984).
30. T. Verkholyak, O. Baran, T. Krokhmalskii, T. Hutak, D. Yaremchuk, and O. Derzhko, *Simple model of magnetoelectric crystal. Dynamic properties, in: The 6th Conference Statistical Physics: Theory and Computer Simulations. 27-29 August 2025, Lviv, Ukraine Dedicated to the 100th Anniversary of Professor Ihor Yukhnovskii. Programme and Abstracts. P. 90* (2025).